LPV Techniques for Control of an Inverted Pendulum

Hiroyuki Kajiwara, Pierre Apkarian, and Pascal Gahinet

Gain-scheduling control structures have proved useful in many practical applications. As an example, most aircraft control laws are based on the interpolation of individually designed controllers or make use of some ad-hoc gain-switching policy. Similarly, in robot control problems the controller dynamics are adjusted in real-time according to geometry and inertias. However, in spite of numerous successful applications, the construction of the overall control structure invariably calls for the engineering insights of the designer and, more critically, the resulting control laws do not provide any guarantees in the face of rapid changes in the scheduled variables. These difficulties have been the main motivation for the development of modern gain-scheduling control techniques, and have led to some challenging research in the area of the analysis and synthesis of LPV systems. Such systems are described in state-space form as

$$\begin{aligned} \dot{x} &= A(\theta)x + B(\theta)u, \\ y &= C(\theta)x + D(\theta)u, \end{aligned} \tag{1}$$

where $\theta := \theta(t)$ is a time-varying parameter describing the range of possible dynamics of the plant. Such systems are natural extensions of customary LTI systems.

Briefly speaking, the recently available LPV synthesis techniques allow the construction of the global control law as a whole entity for all admissible θ, that is, without requiring unnatural separated design syntheses. They furthermore provide theoretical guarantees in terms of both stability and performance in the presence of fast time-domain evolutions of the scheduled variables. Note also that these synthesis techniques reduce to solving a finite set of LMIs (Linear Matrix Inequality), which are easily solved using currently available LMI codes.

In this work, we are considering the challenging application of an arm-driven inverted pendulum (ADIP) as depicted in Fig. 1. The ADIP was originally designed by Dr. Y. Nishi for training purposes at Kawasaki Heavy Industry in Japan. Here the pendulum is the top link and is driven by the rotated arm (bottom link), instead of a more classical cart. As the arm is rotated and gets closer to the horizontal position, the horizontal motion of the arm tip becomes more limited and the inertias viewed from the arm are modified. This naturally leads to the design of controllers that adjust in real-time to the rotation of the arm. For this purpose, two kinds of LPV synthesis techniques are investigated:

Hiroyuki Kajiwara (kajiwara@ces.kyutech.ac.jp) is with the Kyushu Institute of Technology, Kawazu, Japan. Pierre Apkarian is with ONERA-CERT, Toulouse, France. Pascal Gahinet is with The MathWorks, Inc., Natick, MA.

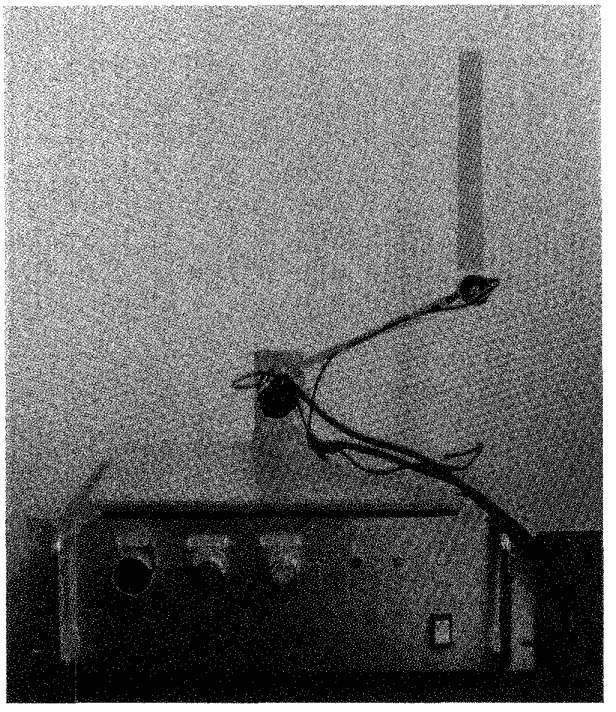

Fig. 1. Arm-driven inverted pendulum (ADIP).

- the so-called LFT (Linear Fractional Transformation) control techniques, which are well suited when the model state-space coefficients are fractional functions of a varying parameter (possibly a state), and
- polytopic techniques, which assume that the state-space coefficients evolve in a prescribed (bounded) polytope (as for instance a hypercube).

The intention behind these different representations is to account for the time-varying and nonlinear nature of the plant by formalizing a set of admissible trajectories instead of a single operating point.

Our aim is to completely validate these techniques on the physical experiment. Therefore, in addition to the usual stability, performance, and robustness requirements, we shall also be concerned by the implementation constraints that inevitably show up in real-world applications. The major implementation constraints are the following.

- The high-frequency gain of the controllers must be compatible with the actuator bandwidth.
- The controller dynamics must be consistent with the available sampling rate in this application ($\leq$1 kHz.).

0272-1708/99/$10.00©1999IEEE

Note that the second of these constraints is especially difficult to handle, as it concerns the internal properties of the controller and cannot be directly treated through the properties of the closed-loop system. We shall see, however, that a suitable multi-objective extension of the polytopic technique provides an effective means to overcome this difficulty. Another way to handle this implementation constraint would have been to tune the weighting functions until adequate closed-loop plant and open-loop controller specifications are met. However, this procedure revealed itself to be intractable in this application and in most instances led to high order controllers, as it requires complicated weighting functions.

Another important issue is to evaluate the benefits of LPV synthesis techniques in regard to classical robust control techniques such as H_∞ and μ syntheses. It turns out in this application that though the H_∞ and μ controllers are capable of providing some stability guarantees they are, as expected, outperformed by LPV controllers at the performance level.

This article is organized as follows. The next section describes the modeling of the ADIP and introduces the problem specifications. A brief review of the LPV synthesis techniques used for the ADIP is given in the following section. The full design procedure up to the nonlinear simulations and real experiment results are then presented, followed by some concluding remarks.

All LMI-related computations in the application were performed using the LMI Control Toolbox [23], μ controllers were designed using the μ-Analysis and Synthesis Toolbox [22], the nonlinear simulations were obtained using MATLAB/SIMULINK facilities and LPV controllers were implemented using the REAL-TIME WORKSHOP.

LPV Modeling of the ADIP

In this section, the LPV synthesis model for the ADIP is developed and the design specifications are introduced. Consider the two-link arm depicted in Fig. 2. It is well known [1], [2] that the motion equation is described as

$$M(q)\ddot{q} + C(q,\dot{q}) + G(q) = \tau, \tag{2}$$

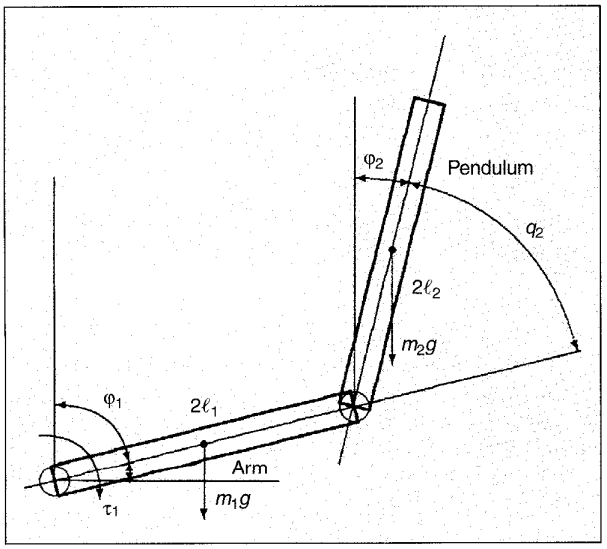

Fig. 2. For modeling of ADIP.

where

$$q = \begin{bmatrix} q_1 \\ q_2 \end{bmatrix} := \begin{bmatrix} \frac{\pi}{2} - \varphi_1 \\ \varphi_1 - \varphi_2 \end{bmatrix} \tag{3}$$

and

$$M(q) := \begin{bmatrix} M_1 + 2R\cos(q_1) & M_2 + R\cos(q_2) \\ M_2 + R\cos(q_2) & M_2 \end{bmatrix} \tag{4}$$

$$M_1 := \frac{4}{3}m_1\ell_1^2 + \frac{4}{3}m_2\ell_2^2 + 4m_2\ell_1^2 \tag{5}$$

$$M_2 := \frac{4}{3}m_2\ell_2^2, \; R := 2m_2\ell_1\ell_2 \tag{6}$$

$$C(q,\dot{q}) := \begin{bmatrix} -2R\dot{q}_1\dot{q}_2\sin(q_2) - R\dot{q}_2^2\sin(q_2) \\ R\dot{q}_1^2\sin(q_2) \end{bmatrix} \tag{7}$$

$$G(q) := \begin{bmatrix} -(m_1 + 2m_2)\ell_1 g\cos(q_1) \\ -m_2\ell_2 g\cos(q_1 + q_2) \end{bmatrix} \tag{8}$$

$$\tau := \begin{bmatrix} -\tau_1 \\ 0 \end{bmatrix}. \tag{9}$$

In this application, the first joint is actuated and the second joint is free. From (2)–(9), we can derive the following equations.

$$\begin{aligned} &(M_1 - M_2)\ddot{\varphi}_1 + R\cos(\varphi_1 - \varphi_2)\ddot{\varphi}_2 \\ &+R\sin(\varphi_1 - \varphi_2)\dot{\varphi}_2^2 + (m_1 + 2m_2)\ell_1 g\sin(\varphi_1) \\ &-m_2\ell_2 g\sin(\varphi_2) = \tau_1, \end{aligned} \tag{10}$$

$$\begin{aligned} &R\cos(\varphi_1 - \varphi_2)\ddot{\varphi}_1 + M_2\ddot{\varphi}_2 - R\sin(\varphi_1 - \varphi_2)\dot{\varphi}_1^2 \\ &-m_2\ell_2 g\sin(\varphi_2) = 0. \end{aligned} \tag{11}$$

The main control objective is to maintain the second arm in a vertical position like an inverted pendulum using the rotation of the (first) actuated arm. In the following, the first arm and the second arm are called *arm* and *pendulum*, respectively. In the physical experiment corresponding to Fig. 2 the arm is actuated by a motor driven by a velocity-control power amplifier. The physical quantities are given as follows:

$$\begin{aligned} &\ell_1 = 0.13\ m, \quad \ell_2 = 0.15\ m, \quad m_1 = 0.05\ kg, \\ &m_2 = 0.03\ kg, \quad g = 9.8\ m/s^2. \end{aligned} \tag{12}$$

As the velocity $\dot{\varphi}_1$ of the first arm can follow the command input voltage u to the amplifier because of the lightness of the second arm, we can assume that the dynamics from the input voltage to the velocity $\dot{\varphi}_1$ is almost equally given by

$$\frac{d}{dt}\dot{\varphi}_1 = -\frac{1}{T_a}\dot{\varphi}_1 + \frac{K_a}{T_a}u. \tag{13}$$

This means that (10) can be simplified to (13) with reasonable accuracy.

On the other hand, (11) becomes

$$2\ell_1\cos(\varphi_1-\varphi_2)\ddot{\varphi}_1+\frac{4}{3}\ell_2\ddot{\varphi}_2=g\sin(\varphi_2)+2\ell_1\sin(\varphi_1-\varphi_2)\dot{\varphi}_1^2. \tag{14}$$

Then, defining

$$r_x := 2\ell_1\sin(\varphi_1),\quad r_y := 2\ell_1\cos(\varphi_1), \tag{15}$$

and using (14), another description for the ADIP is as follows:

$$\cos(\varphi_2)\ddot{r}_x+\frac{4}{3}\ell_2\ddot{\varphi}_2=(g+\ddot{r}_y)\sin(\varphi_2). \tag{16}$$

The pendulum has two kinds of equilibrium states:

- unstable equilibrium state: $\varphi_2^*=0$ (tip pointing upwards)
- stable equilibrium state: $\varphi_2^*=\pi$ (tip pointing downwards).

In this application, we will only consider the difficult situation where the tip is pointing upwards. An immediate linearization of (16) around $\varphi_2^*=0$ then leads to

$$\ddot{r}_x+\frac{4}{3}\ell_2\ddot{\varphi}_2=(g+\ddot{r}_y)\varphi_2. \tag{17}$$

Introducing the new variable z defined as

$$z := r_x+\frac{4}{3}\ell_2\varphi_2, \tag{18}$$

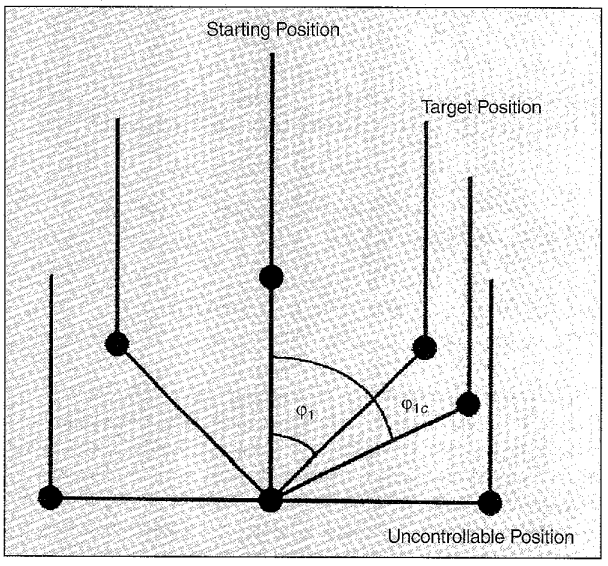

Fig. 3. Wide range stabilization for ADIP.

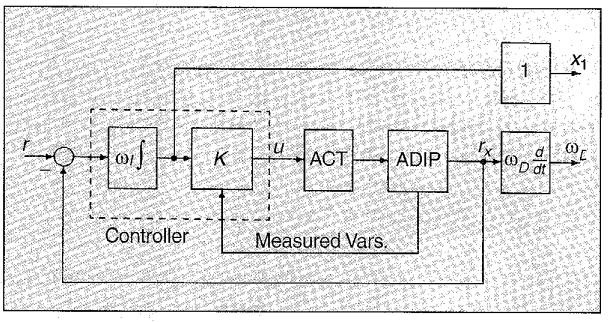

Fig. 4. Interconnection structure for ADIP.

we get

$$\ddot{z}=\frac{3}{4\ell_2}(g+\ddot{r}_y)(z-r_x). \tag{19}$$

Gathering the equation $\dot{r}_x=r_y\dot{\varphi}_1$ with (13) and (19) the following simple LPV model is obtained

$$\frac{d}{dt}\begin{bmatrix} z\\ \dot{z}\\ r_x\\ \dot{\varphi}_1\end{bmatrix}=\left\{\begin{bmatrix}0&1&0&0\\0&0&0&0\\0&0&0&0\\0&0&0&-\frac{1}{T_a}\end{bmatrix}+\frac{3}{4\ell_2}(g+\ddot{r}_y)\begin{bmatrix}0\\1\\0\\0\end{bmatrix}\begin{bmatrix}1&0&-1&0\end{bmatrix}+r_y\begin{bmatrix}0\\0\\1\\0\end{bmatrix}\begin{bmatrix}0&0&0&1\end{bmatrix}\right\}\begin{bmatrix} z\\ \dot{z}\\ r_x\\ \dot{\varphi}_1\end{bmatrix}+\begin{bmatrix}0\\0\\0\\\frac{K_a}{T_a}\end{bmatrix}u, \tag{20}$$

where both z and r_x are assumed to be measured, r_y is viewed as an external time-varying parameter, and $\ddot{r}_y$ is assumed to be zero because its value is negligible in face of g around the vertical line ($\varphi_1<60°$). Moreover, as we have already experimented, scheduling $\ddot{r}_y$ does not bring any improvement in the design and our assumption substantially simplifies the derivation hereafter.

In order to derive LPV models with bounds on the time-varying parameters, it is assumed that the arm can rotate within the angular range

$$-\overline{\varphi}_1\le\varphi_1\le\overline{\varphi}_1\quad\left(0<\overline{\varphi}_1<\frac{\pi}{2}\right). \tag{21}$$

This yields upper ($\overline{r_y}$) and lower ($\underline{r_y}$) for the range of variation of r_y:

$$r_y\in[\underline{r_y},\overline{r_y}] := [2\ell_1\cos(\overline{\varphi}_1),2\ell_1\cos(0)]. \tag{22}$$

From (22), r_y is normalized as

$$\theta_r := \frac{2}{\overline{r_y}-\underline{r_y}}\left(r_y-\frac{\overline{r_y}+r_y}{2}\right)\in[-1,1]. \tag{23}$$

Two different—though completely equivalent—LPV representations can be used for the ADIP. This is described in the sequel.

LPV model with LFT structure

In LFT representations, the parameter or state dependence of the plant state-space matrices is reformulated as an outer loop closed on a nominal plant, which involves the parameter in multiplicative form. Representing r_y from (23) as

$$\begin{aligned} r_y &= \frac{\overline{r_y}+r_y}{2}+\frac{\overline{r_y}-r_y}{2}\theta_r\\ &= \ell_1(1+\cos(\overline{\varphi}_1))+\ell_1(1-\cos(\overline{\varphi}_1))\theta_r, \end{aligned} \tag{24}$$

where θ_r denotes the new normalized scheduling variables, the following LPV model of LFT type is obtained:

$$\frac{d}{dt}\begin{bmatrix} z \\ \dot{z} \\ r_x \\ \dot{\varphi}_1 \end{bmatrix} = \begin{bmatrix} 0 & 1 & 0 & 0 \\ \frac{3g}{4\ell_2} & 0 & -\frac{3g}{4\ell_2} & 0 \\ 0 & 0 & 0 & \frac{\overline{r_y}+\underline{r_y}}{2} \\ 0 & 0 & 0 & -\frac{1}{T_a} \end{bmatrix} \begin{bmatrix} z \\ \dot{z} \\ r_x \\ \dot{\varphi}_1 \end{bmatrix} + \begin{bmatrix} 0 \\ 0 \\ \frac{\overline{r_y}-\underline{r_y}}{2} \\ 0 \end{bmatrix} w_r + \begin{bmatrix} 0 \\ 0 \\ 0 \\ \frac{K_a}{T_a} \end{bmatrix} u \tag{25}$$

$$z_r = [\,0 \;\; 0 \;\; 0 \;\; 1\,] \begin{bmatrix} z \\ \dot{z} \\ r_x \\ \dot{\varphi}_1 \end{bmatrix} \tag{26}$$

with

$$w_r = \theta_r z_r \quad (|\theta_r(t)| \le 1). \tag{27}$$

LPV Model with Polytopic Structure

In polytopic descriptions, the matrix coefficients are expressed as convex combinations of their extreme values. Hence, similarly to the above, by remarking that

$$\frac{\overline{r_y}-r_y}{\overline{r_y}-\underline{r_y}} + \frac{r_y-\underline{r_y}}{\overline{r_y}-\underline{r_y}} = 1, \tag{28}$$

and introducing the notation

$$\rho_1(r_y) := \frac{\overline{r_y}-r_y}{\overline{r_y}-\underline{r_y}}, \quad \rho_2(r_y) := \frac{r_y-\underline{r_y}}{\overline{r_y}-\underline{r_y}}, \tag{29}$$

we obtain the following LPV polytopic model for the ADIP:

$$\frac{d}{dt}\begin{bmatrix} z \\ \dot{z} \\ r_x \\ \dot{\varphi}_1 \end{bmatrix} = \left(\rho_1(r_y) \begin{bmatrix} 0 & 1 & 0 & 0 \\ \frac{3g}{4\ell_2} & 0 & -\frac{3g}{4\ell_2} & 0 \\ 0 & 0 & 0 & \overline{r_y} \\ 0 & 0 & 0 & -\frac{1}{T_a} \end{bmatrix} + \rho_2(r_y) \begin{bmatrix} 0 & 1 & 0 & 0 \\ \frac{3g}{4\ell_2} & 0 & -\frac{3g}{4\ell_2} & 0 \\ 0 & 0 & 0 & \underline{r_y} \\ 0 & 0 & 0 & -\frac{1}{T_a} \end{bmatrix} \right) \begin{bmatrix} z \\ \dot{z} \\ r_x \\ \dot{\varphi}_1 \end{bmatrix} + \begin{bmatrix} 0 \\ 0 \\ 0 \\ \frac{K_a}{T_a} \end{bmatrix} u, \tag{30}$$

and it is easily verified that ρ_1 and ρ_2 are polytopic coordinates, that is, $\rho_1 \ge 0$ and $\rho_2 \ge 0$ and $\rho_1 + \rho_2 = 1$.

Quick Look at the Wide-Range Stabilization Problem

As already stated, the main control objective for the ADIP is to stabilize the inverted pendulum using the rotations of the arm, as depicted in Fig. 3 below, and simultaneously increase (as much as possible) the range where stabilization is achieved. One important difficulty of this problem comes from the fact that the ADIP becomes uncontrollable as the pendulum gets closer to the horizontal position, hence the need for a gain-scheduled controller. Apart from the maximization of the range where stabilization holds, we must also provide performance in terms of settling-time and overshoot in response to reference signals. This will be detailed in a later section. Also the controller should exhibit adequate roll-off in the high-frequency range for noise attenuation.

LPV Control Techniques

This section provides a brief review of the design techniques that will be used for the ADIP application. Two LPV design techniques will be investigated:

- the LFT design technique,
- the polytopic design technique.

As indicated by their names, such techniques apply to LPV plants with LFT and polytopic parameter-dependence, respectively. The first class of LPV plants can be described as

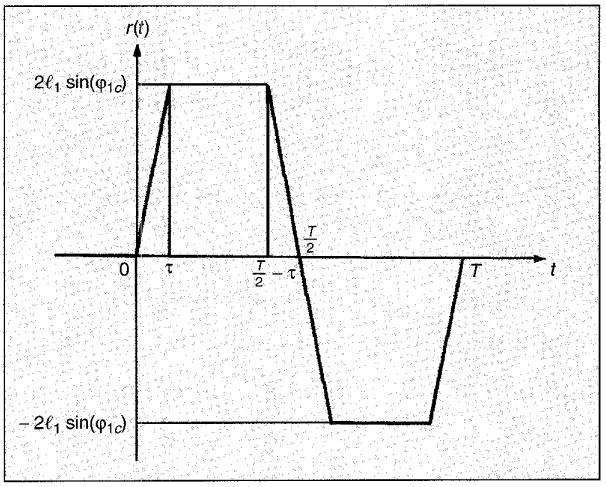

Fig. 5. Reference signal r to r_x.

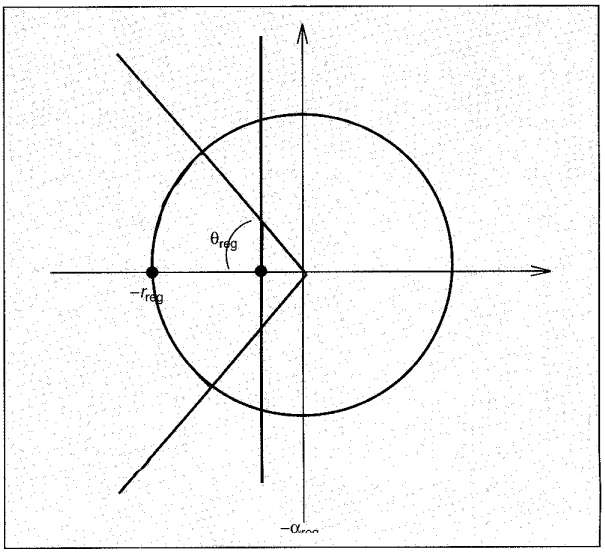

Fig. 6. LMI region for closed-loop system.

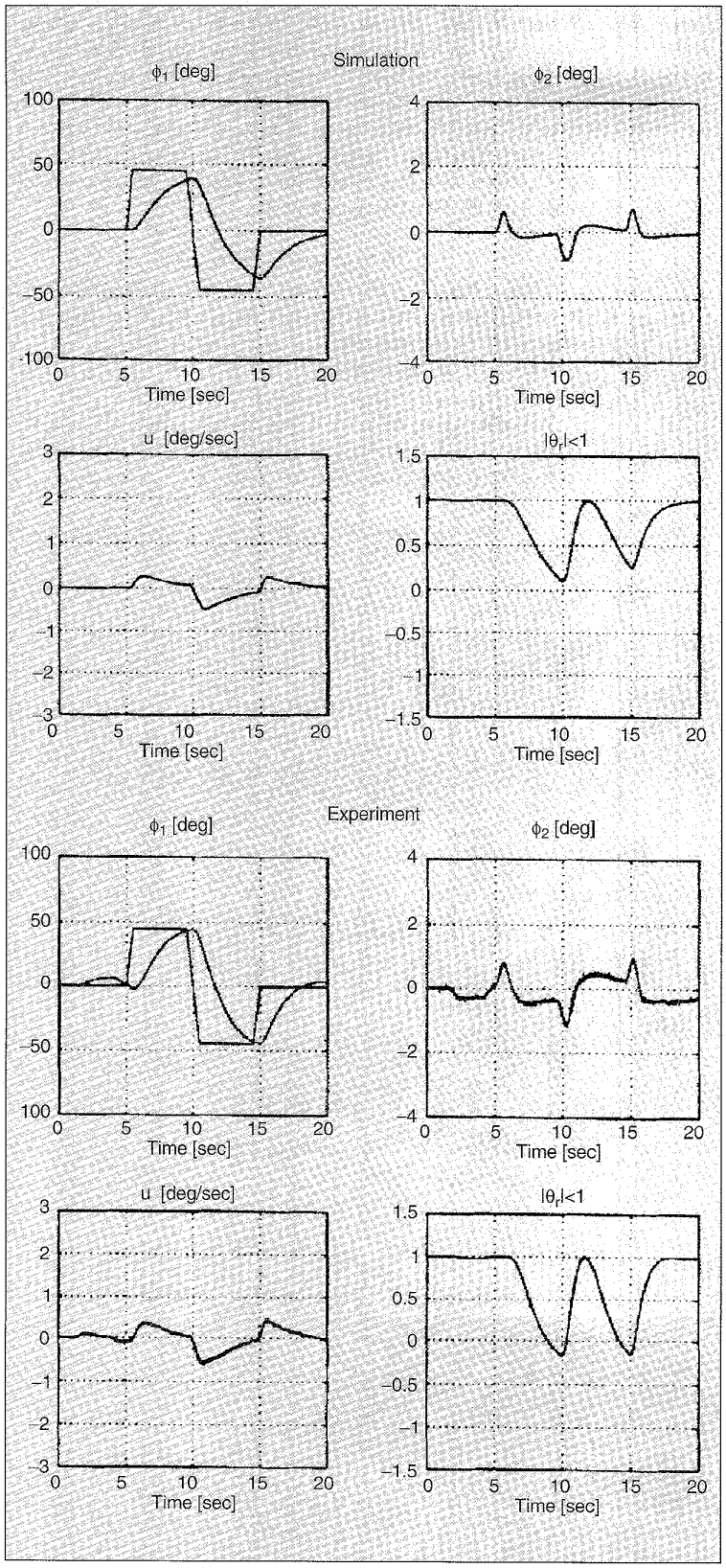

Fig. 7. H_∞ Control results ($\gamma = 2.5774$, $\varphi_{1c} = 45°$).

$$\begin{aligned} \dot{x} &= Ax + B_\theta w_\theta + B_1 w + B_2 u, \\ z_\theta &= C_\theta x + D_{\theta\theta} w_\theta + D_{\theta 1} w + D_{\theta 2} u, \\ z &= C_1 x + D_{1\theta} w_\theta + D_{11} w + D_{12} u, \\ y &= C_2 x + D_{2\theta} w_\theta + D_{21} w + D_{22} u, \\ w_\theta &= \Theta(t)\, z_\theta, \end{aligned} \tag{31}$$

where $\Theta(t)$ is a time-varying parameter matrix and is usually assumed to have a block-diagonal structure in the form

$$\Theta(t) = \mathrm{diag}(\ldots, \Theta_i(t), \ldots, \theta_j(t) I, \ldots), \tag{32}$$

and is normalized such that

$$\Theta(t)^T \Theta(t) \le I, \quad t \ge 0. \tag{33}$$

Blocks denoted Θ_i and $\theta_j\, I$ are generally referred to as full and repeated-scalar blocks according to the μ analysis and synthesis literature [3], [4]. Note that straightforward computations lead to the state-space representation

$$\begin{bmatrix} \dot{x} \\ z \\ y \end{bmatrix} = \left\{ \begin{bmatrix} A & B_1 & B_2 \\ C_1 & D_{11} & D_{12} \\ C_2 & D_{21} & D_{22} \end{bmatrix} + \begin{bmatrix} B_\theta \\ D_{1\theta} \\ D_{2\theta} \end{bmatrix} \Theta(t) \right. \times \left. (I - D_{\theta\theta}\Theta(t))^{-1} [C_\theta \; D_{\theta 1} \; D_{\theta 2}] \right\} \begin{bmatrix} x \\ w \\ u \end{bmatrix}, \tag{34}$$

hence the plant with inputs w and u and outputs z and y has state-space data entries which are fractional functions of the time-varying parameter $\Theta(t)$. Hereafter, we are using the following notation

- u for the control signal
- w for exogenous inputs
- z for controlled or performance variables
- y for the measurement signal.

As an alternative to this description, we are also considering polytopic systems which are described by the state-space representation

$$\begin{aligned} \dot{x} &= A(\rho(t))x + B_1(\rho(t))w + B_2(\rho(t))u, \\ z &= C_1(\rho(t))x + D_{11}(\rho(t))w + D_{12}(\rho(t))u, \\ y &= C_2(\rho(t))x + D_{21}(\rho(t))w + D_{22}(\rho(t))u, \end{aligned} \tag{35}$$

where generally, $A(\rho)$, $B_1(\rho)$,... are affine functions of the time-varying parameter $\rho(t)$ evolving in a polytopic set $\mathcal{P}_\rho$, i.e.,

$$\rho(t) \in \mathcal{P}_\rho := \mathrm{co}\{\rho_{v_1}, \ldots, \rho_{v_r}\}, \quad t \ge 0, \tag{36}$$

where the notation co{.} stands for the convex hull of the set {.}.

Clearly, the state-space data of the plant (35) range over a matrix polytope and thus it trivially holds that

$$\begin{bmatrix} A(\rho(t)) & B_1(\rho(t)) & B_2(\rho(t)) \\ C_1(\rho(t)) & D_{11}(\rho(t)) & D_{12}(\rho(t)) \\ C_2(\rho(t)) & D_{21}(\rho(t)) & D_{22}(\rho(t)) \end{bmatrix} \in P$$
$$:=\text{co}\left\{\begin{bmatrix} A_i & B_{1i} & B_{2i} \\ C_{1i} & D_{11i} & D_{12i} \\ C_{2i} & D_{21i} & D_{22i} \end{bmatrix}, i=1,2,...,r\right\}, \quad (37)$$

where

$$\begin{bmatrix} A_i & B_{1i} & B_{2i} \\ C_{1i} & D_{11i} & D_{12i} \\ C_{2i} & D_{21i} & D_{22i} \end{bmatrix} := \begin{bmatrix} A(\rho_{v_i}) & B_1(\rho_{v_i}) & B_2(\rho_{v_i}) \\ C_1(\rho_{v_i}) & D_{11}(\rho_{v_i}) & D_{12}(\rho_{v_i}) \\ C_2(\rho_{v_i}) & D_{21}(\rho_{v_i}) & D_{22}(\rho_{v_i}) \end{bmatrix},$$
$$i=1,...,r. \quad (38)$$

For any of the LPV plants (31)-(33) or (35)-(37), the LPV control problem (often referred to as the gain-scheduling control problem) consists in seeking an LPV controller

$$\dot{x}_K = A_K(p)x_K + B_K(p)y,$$
$$u = C_K(p)x_K + D_K(p)y, \quad (39)$$

where $p(t) = \Theta(t)$ for the LFT-LPV plant (31)-(33) and $p(t) = \rho(t)$ for the polytopic LPV plant (35)-(37) such that

- the closed-loop system (31)–(33) and (39) or the closed-loop system (35)–(37) and (39) is internally stable,
- the L_2-induced gain of the operator connecting w to z is bounded by γ,

for all parameter trajectories $p(t)$ defined by either (33) or (37).

It is now well-known that such problems can be handled via a suitable generalization of the Bounded Real Lemma and can be solved by computing solutions to a set of LMIs. It is important to note that LMI problems are convex and thus one can easily compute a solution to these problems (whenever it exists) by using very efficient codes of semi-definite programming [14]-[17].

Controller Implementation Constraints

Using a more general approach, it is possible to characterize multiple and multi-channel specifications in the case of polytopic LPV systems [10], [19], [9]. Since it has proven useful in the ADIP control problem, we briefly discuss the LMIs characterizing L_2-gain performance in conjunction with LMI region constraints on the poles of the closed-loop system. The reader is referred to [19] and [20] for a thorough discussion on LMI regions and their use in robust control theory and to the web reference [24] for a de-

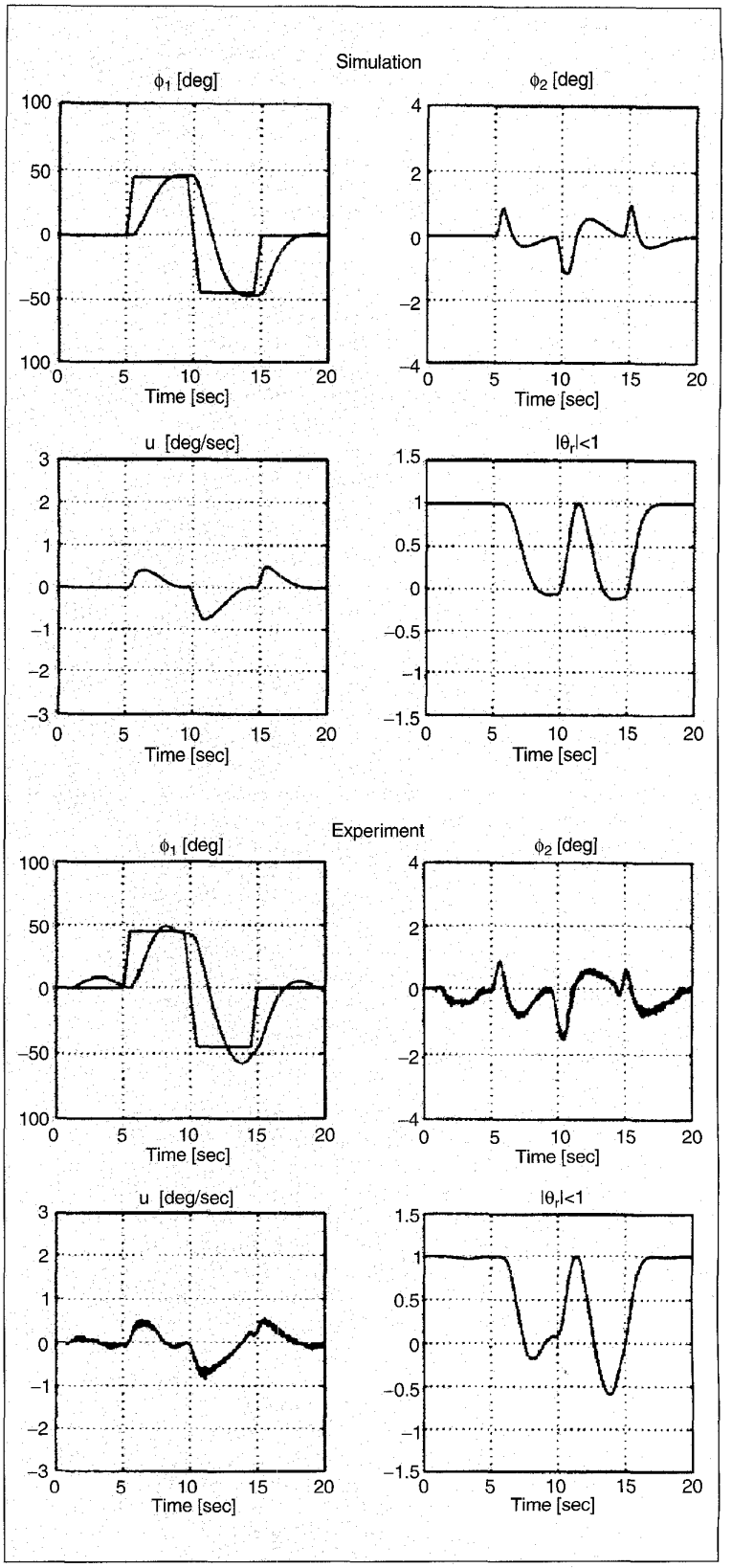

Fig. 8. μ Control results ($\gamma = 0.7938$, $\varphi_{1c} = 45°$).

tailed description of the LMI characterizations involved. LMI regions are self-conjugate regions of the complex plane which are useful to specify transient constraints for the closed-loop dynamics. Interesting examples of such regions include vertical and horizontal strips, circles, conic sectors, etc., and their intersections thereof which again are LMI regions (see Fig. 6 for an illustration). Moreover, any self-conjugate region of the complex plane can be approximated to any desired accuracy with an LMI region.

Another practical advantage of LMI region constraints is that they can be exploited to indirectly enforce constraints on the controller dynamics and thus on the controller bandwidth. This is of primary importance in any realistic design. We stress here that such an approach is only indirect and might require preliminary adjustments and trials to translate original constraints on the controller into constraints on the closed-loop dynamics. These adjustments are useful to avoid unnecessary restrictions on the design problem. From a theoretical viewpoint, achieving controller bandwidth specifications remains a delicate and unsolved question, except for some classes of fixed-structure controllers such as PID and the like. In the context of this paper, it is enough to have in mind that LMI region constraints provide a sensible though not direct approach to this problem. A more abstract justification can be found in [19].

This approach extends naturally to polytopic plants in (35) but does not have yet any counterpart for LFT plants (31) (see [24]). Also important is the fact that pole constraints must be understood in the time-invariant sense, that is, for "frozen" values of the parameter in its range. Obviously, these concepts must be handled with care when one manipulates the time-varying plants described previously. In the ADIP application, stability and performance are time-variant specifications whereas LMI region constraints are classical time-invariant pole constraints. It is shown that the formulation is powerful enough to meet the implementation constraints of our application.

When solutions to the LMI conditions have been found, the state-space data of the controller in (39) can be computed for any admissible value of the parameter $\Theta(t)$ or $\rho(t)$, using well-known schemes. The reader is referred to [18] and [21], and to [7]–[9], for a comprehensive discussion.

LPV Controller Synthesis for the ADIP

In this section, we first give a thorough description of the specifications and control objectives together with the control structure used for the ADIP. Next different robust and LPV syntheses are carried out and results are discussed with regard to the specifications introduced earlier but also from the viewpoint of the ease of implementation on the physical experiment. This last phase has been found necessary since we have observed some mismatches between computerized nonlinear simulations and the "real" responses on the ADIP.

Problem Presentation and Specifications

For the designs, we shall be using the synthesis interconnection shown in Fig. 4. The serial connection of the ADIP and the actuator (ACT) is described by (25)–(27) or (29)–(30) depending on the particular LPV representation we are actually using. Note that we have introduced some integral action in the forward channel to ensure zero steady-state tracking error at an equilibrium position. The integral action is here described as

$$\dot{x}_I = \omega_I (r - r_x), \tag{40}$$

where ω_I is a design parameter. The family of test or reference signals r for the arm rotation in the range (21) which are used hereafter can be described as follows.

$$r(t) := \begin{cases} \frac{r_{\max}}{\tau} t & (0 \le t \le \tau) \\ r_{\max} & (\tau \le t \le \frac{T}{2} - \tau) \\ -\frac{r_{\max}}{\tau}(t - \frac{T}{2}) & (\frac{T}{2} - \tau \le t \le \frac{T}{2} + \tau) \\ -r_{\max} & (\frac{T}{2} + \tau < t < T - \tau) \\ \frac{r_{\max}}{\tau}(t - T) & (T - \tau \le t \le T), \end{cases} \tag{41}$$

where $r_{\max} := 2\ell_1 \sin(\varphi_{1c})$, $\tau = 0.5$ and $\varphi_{1c} (\le \overline{\varphi}_1)$ is a target value. A simple drawing of such signals is depicted in Fig. 5. Then the specifications for the control system are the following:

(S1) the closed-loop system is internally stable.

(S2) the L_2-induced gain of the operator connecting $w = r$ to $z = \begin{bmatrix} \omega_D \dot{r} \\ x_I \end{bmatrix}$ is bounded by γ, where ω_D is a design parameter.

(S3) specifications **(S1)** and **(S2)** must hold on the largest range of $\overline{\varphi}_1$ as far as possible.

(S4) the LPV controller must be implementable with a minimum sampling interval 1 msec.

The specification **(S1)** means that the LPV controller must stabilize the inverted pendulum in any vertical position in the

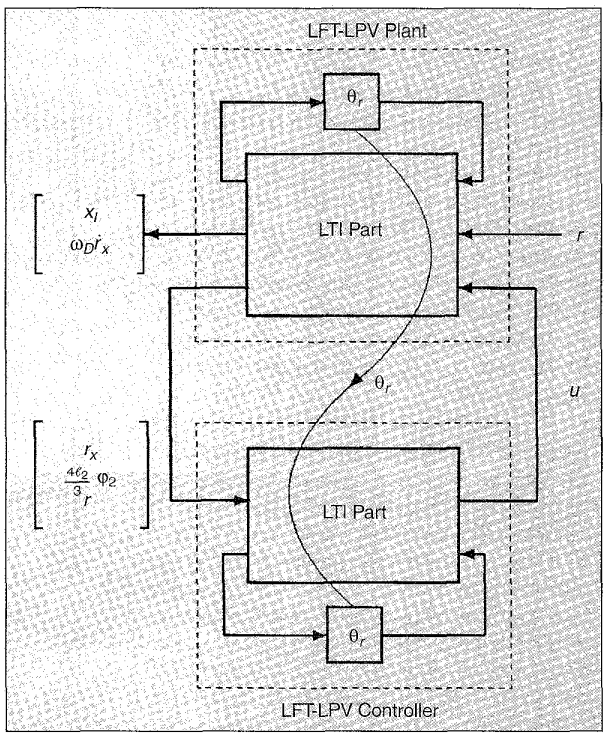

Fig. 9. LPV control with LFT structure.

range $\varphi_1 \in [-\overline{\varphi}_1, \overline{\varphi}_1]$. Specification **(S2)** translates performance tracking and high-frequency gain attenuation objectives. The specification **(S3)** express that stabilization but also performance and roll-off requirements must be achieved on the largest range of possible dynamics of the ADIP. The specification **(S4)** is directly dictated from physical hardware limitations.

Robust LTI Syntheses

Before utilizing the LPV synthesis techniques introduced in the previous section, it is instructive to investigate what can be achieved using customary robust control techniques such as H_∞ and μ syntheses. Note first that since the synthesis problem depicted in Fig. 4 is completely singular ($D_{12} = 0$ and $D_{21} = 0$), any H_∞ synthesis steps were performed using the LMI formulation in [19], which is not restricted by singularity problems. Moreover, in order to satisfy the implementation constraints **(S4)**, which require reasonable controller dynamics, we also have introduced LMI region pole constraints on the closed-loop dynamics. This requires using the refined H_∞ synthesis technique in [19] (see also the prior section). The LMI region under consideration is determined by the intersection of a half-plane, a conic sector and a disk, as shown in Fig. 6.

H_∞ synthesis based on a nominal model

Based on a nominal model (ADIP in vertical position $\varphi_1 = 0$, i.e. $\overline{\varphi}_1 = 0$), an H_∞ controller has been computed leading to a performance level $\gamma = 2.5774$ where the $\omega_D = 0.02, \omega_I = 0.5$ and the LMI region constraint is determined by $\alpha_{reg} = 0.5$, $r_{reg} = 50, \theta_{reg} = 45°$. The poles of the H_∞ controller are given as

$$\{-67.166, -49.834 \pm 19.109j, -39.3169, -0.1319, 0\}.$$

Note that this is in stark contrast with the result obtained without pole constraints which yielded the controller poles

$$\{-3.3110 \times 10^5, -5.8209 \times 10^4, -3.97759 \times 10^4, -2.0037 \times 10^4, -22.806, 0\}.$$

Such dynamics clearly do not satisfy the implementation constraints **(S4)** and thus must be ruled out in this application. So, we only retained the first H_∞ controller. The corresponding nonlinear simulations using the realistic model (2) are compared with records on the "true" experiment in Fig. 7. For each figure, the (1,1)-subplot shows the command and the time-response of φ_1, the (1,2)-subplot shows φ_2, the (2,1)-subplot shows the control signal u, and the (2,2)-subplot shows θ_r. We first observe the consistency of the responses of the simulation and the experiment, which to some extent validates the simplified model we have used for synthesis. One can also see that the control sys-

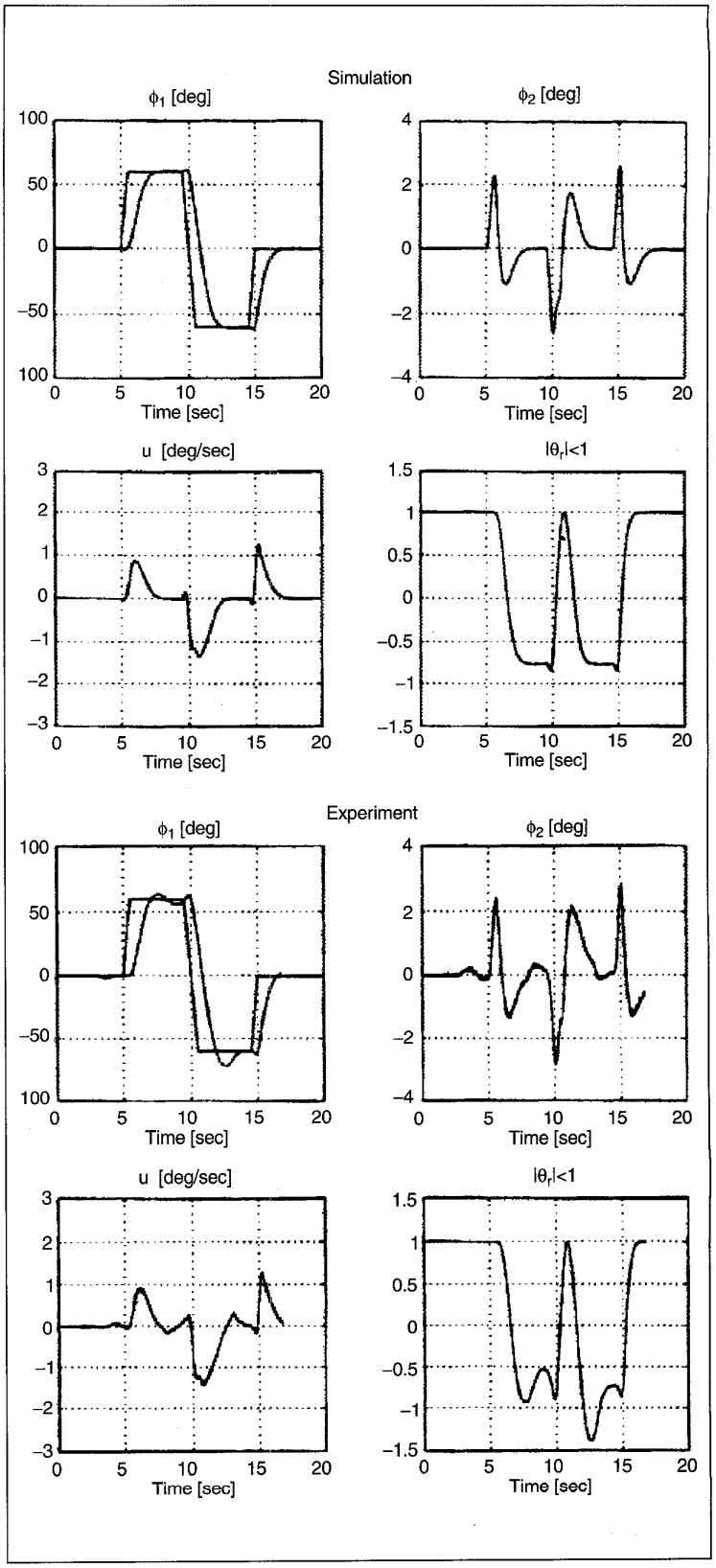

Fig. 10. LFT Control results ($\gamma = 0.4733$, $\varphi_{1c} = 60°$).

tem has very poor performance using this controller even on the somewhat reduced target $\varphi_{1c} = 45°$.

μ *Controller Based on an Uncertain Model*

We decided to improve these preliminary results using μ synthesis by explicitly taking account of the changing dynamics of the ADIP, where $\overline{\varphi}_1 = 65°$. We have used first-order μ scaling and the parameters were tuned to $\omega_D = 0.02, \omega_I = 0.8$ and $\alpha_{reg} = 0.1$, $r_{reg} = 50$, $\theta_{reg} = 45°$. With the H_∞ synthesis steps enforcing closed-loop pole constraints, we obtained some controllers with poles

$$\{-61.497 \pm 25.596\,j, -47.080, -33.753, \\ -0.8993, -0.3723, -0.2206, 0\},$$

which are clearly satisfactory with respect to the implementation constraints. In our example, usual μ synthesis algorithms would lead to unacceptable controller dynamics. As before, the nonlinear simulations and the hardware experiment are shown in Fig. 8.

As expected, this second controller provides better performance on the target $\varphi_{1c} = 45°$. However, the very same controller but with the target φ_{1c} increased to 60° does not even provide stability and we did not find any simple way to guarantee the same level of performance on this larger range.

Summing up our results, the H_∞ controller is able to stabilize the range 45° but provides very poor performance. The μ controller provides adequate performance on the range 45° but no longer works for ranges up to 60°, illustrating a fundamental tradeoff between performance and the size of the operating range. In many applications this tradeoff is very limiting and can only be negotiated outside the set of fixed controller structures by exploiting gain-scheduling strategies. This is considered in the next section.

LPV Syntheses

In this section, the synthesis techniques discussed in previously are exploited to improve both performance and the operating range of the ADIP.

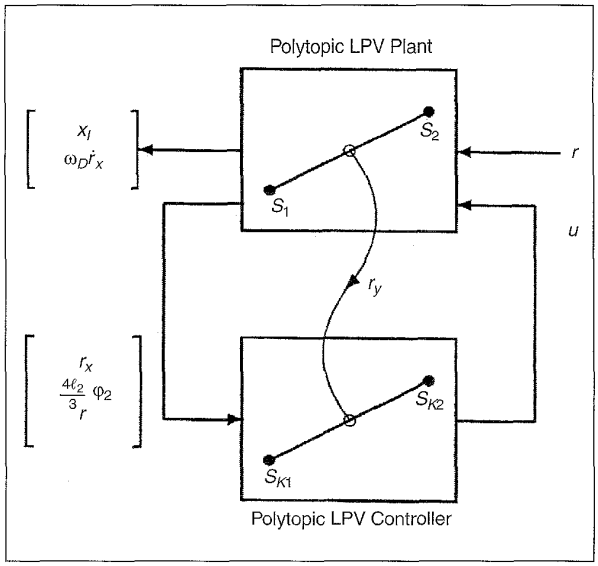

Fig. 11. LPV control with polytopic structure.

Design of an LFT Controller

An LPV control system with LFT structure is depicted in Fig. 9. An LFT-LPV controller

$$\begin{bmatrix} A_K(\rho(t)) & B_K(\rho(t)) \\ C_K(\rho(t)) & D_K(\rho(t)) \end{bmatrix} = \begin{bmatrix} A_K & B_K \\ C_K & D_K \end{bmatrix} + \\ \begin{bmatrix} B_{K\Theta} \\ D_{K\Theta\bullet} \end{bmatrix} \Theta(t)(I - D_{K\Theta\Theta}\Theta(t))^{-1} \begin{bmatrix} C_{K\Theta} & D_{K\bullet\Theta} \end{bmatrix} \tag{42}$$

is designed using the LFT description of the ADIP, where $\overline{\varphi}_1 = 65°$. The parameters ω_D and ω_I were set to 0.02 and 0.5, respectively. The underlying LTI dynamics of the LFT controller are easily obtained by instantiating the LFT controller at some frozen values of θ_r. For the extreme values of θ_r the following dynamics are obtained.

$$\theta_r = 1: \{-365.56, -359.74, -291.81, \\ -24.064, -1.3786, 0\},$$

$$\theta_r = -1: \{-365.56, -359.72, -291.84, \\ -42.888, -1.4367, 0\}.$$

Such dynamics are again satisfactory in regard to implementation constraints and have been derived by minimizing, through an LMI formulation, the norm of the A matrix of the LPV controller in the construction procedure. The nonlinear simulations and the hardware experiments are shown in Fig. 11. As expected, both performance and the the size of the operating range have been enhanced as compared to previous LTI controllers.

Design of a Polytopic Controller

An LPV control system with polytopic structure is depicted in Fig. 11. A similar design is now conducted using the polytopic description of the ADIP, where $\overline{\varphi}_1 = 65°$, leading to polytopic LPV controllers

$$\begin{bmatrix} A_K(\rho(t)) & B_K(\rho(t)) \\ C_K(\rho(t)) & D_K(\rho(t)) \end{bmatrix} = \\ \rho_1(t) \underbrace{\begin{bmatrix} A_{K1} & B_{K1} \\ C_{K1} & D_{K1} \end{bmatrix}}_{S_{K1}} + \rho_2(t) \underbrace{\begin{bmatrix} A_{K2} & B_{K2} \\ C_{K2} & D_{K2} \end{bmatrix}}_{S_{K2}}. \tag{43}$$

In order to satisfy the implementation constraints (**S4**), we have used a refined synthesis technique which can handle constraints on the closed-loop dynamics. With the selection $\omega_D = 0.1$, $\omega_I = 0.5$ and $\alpha_{reg} = 1$, $r_{reg} = 50$, $\theta_{reg} = 45°$, the underlying LTI controllers obtained at the extreme values of the parameter range have the following dynamics

$$\varphi_1 = 0°: \{-69.352 + -50.251\,j, -53.529, \\ -20.775, -3.6379, 0\},$$

$$\varphi_1 = 65°: \{-76.0805, -35.506 \pm 41.303\,j, \\ -35.159, -2.1349, 0\}.$$

They are again satisfactory. The nonlinear simulations and the hardware experiments with the polytopic controller are shown in Fig. 12. It is again observed that very good performance is achieved over the same operating range.

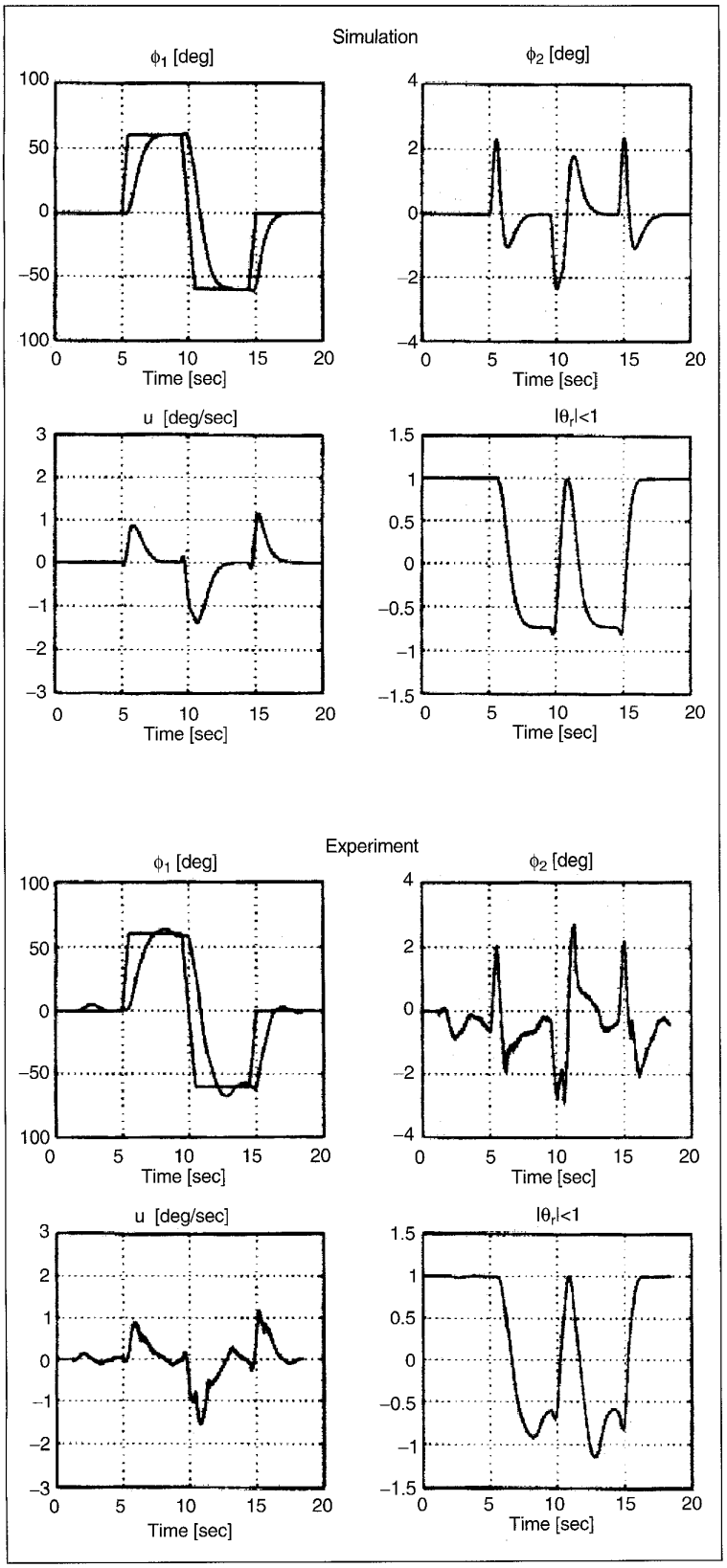

Fig. 12. Polytopic control results ($\gamma = 0.4729$, $\varphi_{1c} = 60°$).

Concluding Remarks

We can summarize the results of the four kinds of synthesis methods as shown in Table 1.

This shows that each synthesis method can theoretically stabilize the operating range $[-\overline{\varphi}_1, \overline{\varphi}_1]$ but experimentally achieves only $[-\varphi_{1c}, \varphi_{1c}]$. As for the μ-synthesis, we observe some gap between the two range, that is, $\overline{\varphi}_1 = 65°$ and $\varphi_{1c} = 45°$. This comes from the model approximation used in the syntheses. In Table 1, T_s indicates the settling times in the experiments.

A quick view of the merits and drawbacks of each technique is presented in Table 2.

Finally, we have presented a comprehensive application of LPV control techniques to the control of an arm-driven inverted pendulum. The particular interest of this application lies in the fact that all ingredients of the design problem have to be taken into account, from the specifications up to the constraints inherent to real-world implementations. In this context, it has been shown that currently available synthesis methodologies, such as μ and LPV techniques, may fail to provide acceptable answers. A major obstacle is undoubtly the implementation constraint that puts hard limitations on the controller dynamics. These limitations are generally difficult to handle within the usual formulation of LPV control techniques.

It has been shown that a suitable extension of these techniques including LMI region constraints on the closed-loop dynamics can overcome this difficulty. When implementable, it has been observed that LPV controllers outperform fixed μ controllers both in robustness and performance. These observations were confirmed by simulations but more importantly by a number of records on the physical experiment.

References

[1] M.W. Spong and M. Vidyasagar, *Robot Dynamics and Control*, Wiley, 1989.

[2] C. Canudas de Wit, B. Siciliano, and G. Bastin (eds.), *The Theory of Robot Control*, Springer, 1996.

[3] M.K.H. Fan, A.L. Tits, and J.C. Doyle, "Robustness in the Presence of Mixed Parametric Uncertainty and Unmodelized Dynamics," *IEEE Trans. Automat. Contr.*, vol. AC-36, no. 1, pp. 25-38, 1991.

[4] J.C. Doyle, A. Packard, and K. Zhou, "Review of LFT's, LMI's and μ," *CDC Brighton, England*, pp. 1227-1232, 1991.

[5] A. Packard and G. Becker, "Quadratic Stabilization of Parametrically-Dependent Linear Systems using Parametrically-Dependent Linear, Dynamic Feedback," *Advances in Robust and Nonlinear Control Systems*, vol. DSC-43, pp. 29-36, 1992.

[6] A. Packard, "Gain Scheduling via Linear Fractional Transformations, *Syst. Contr. Lett.*, vol. 22, no. 2, pp. 79-92, 1994.

Table 1. Performance indexes for LTI and LPV methods				
Synthesis	γ	$\overline{\varphi}_1$	φ_{1c}	T_s
H_∞	2.57	–	45°	5s
μ	0.79	65°	45°	2.5s
LFT-LPV	0.47	65°	60°	2s
Poly-LPV	0.42	65°	60°	2s

Table 2. Merits and drawbacks in LTI and LPV methods	
Synthesis	Comments
H_∞	less performance needs pole constraint
μ	often higher order needs pole constraint
LFT-LPV	no direct pole constraint can handle general θ-dependence
Poly-LPV	pole constraint OK restricted to affine θ-dependence

[7] P. Apkarian and P. Gahinet, "A Convex Characterization of Gain-Scheduled H_∞ Controllers," *IEEE Trans. Automat. Contr.*, vol. 40, no. 5, pp. 853-864, 1995.

[8] P. Apkarian, P. Gahinet, and G. Becker, "Self-Scheduled H_∞ Control of Linear Parameter-Varying Systems: A Design Example," *Automatica*, vol. 31, no. 9, pp. 1251-1261, 1995.

[9] P. Apkarian and R.J. Adams, "Advanced Gain-Scheduling Techniques for Uncertain Systems," *IEEE Trans. on Control System Technology*, to appear, 1998.

[10] C. Scherer, "Mixed H_2 / H_∞ Control," *Trends in Control: A European Perspective*, volume of the Special Contribution to the ECC 95.

[11] C. Scherer, "Mixed H_2 / H_∞ Control for Linear Parametrically Varying Systems," *CDC New Orleans, LA*, pp. 3182-3187, 1995.

[12] G. Scorletti and L. El. Ghaoui, "Improved Linear Matrix Inequality Conditions for Gain-Scheduling," *CDC New Orleans, LA*, pp. 3626-3631, 1995.

[13] A. Helmersson, "Methods for Robust Gain-Scheduling," Ph. D. Thesis, Linkoping University, Sweden, 1995.

[14] Yu. E. Nesterov and A.S. Nemirovski, "Interior Point Polynomial Methods in Convex Programming: Theory and Applications," *SIAM Studies in Applied Mathematics* vol. 13, SIAM, 1994.

[15] L. Vanderberghe and S. Boyd, "Primal-Dual Potential Reduction Method for Problems Involving Matrix Inequalities," *Math. Programming Series B*, no. 69, pp. 205-236, 1995.

[16] S. Boyd and L. El. Ghaoui, "Method of Centers for Minimizing Generalized Eigenvalues," *Lin. Alg. and Applic.*, vol. 188, pp. 63-111, 1992.

[17] P. Gahinet and A. Nemirovski, "General-Purpose LMI Solvers with Benchmarks," *CDC San Antonio*, pp. 3162-3165, 1993.

[18] P. Gahinet and P. Apkarian, "A Linear Matrix Inequality Approach to H_∞ Control," *Int. J. Robust and Nonlinear Contr.*, vol. 4, pp. 421-448, 1994.

[19] M. Chilali and P. Gahinet, "H_∞ Design with Pole Placement Constraints: an LMI Approach," *IEEE Trans. Autom. Contr.*, vol. 41, 3, pp. 358-367, 1996.

[20] G. Garcia, D. Arzelier, J. Daafouz, and J. Bernussou, "An {LMI} Formulation for Robust Disk Pole Assignment via Output Feedback," *IFAC World Congress*, San Fransisco, 1996

[21] T. Iwasaki and R.E. Skelton, "All Controllers for the General H_∞ Control Problem: LMI Existence Conditions and State Space Formulas," *Automatica*, vol. 30, no. 8, pp. 1307-1317, 1994.

[22] G.J. Balas, J.C. Doyle, K. Glover, A. Packard, and R. Smith, "μ-Analysis and Synthesis Toolbox," The MathWorks, 1993.

[23] P. Gahinet, A. Nemirovski, A.J. Laub, and M. Chilali, "LMI Control Toolbox," The MathWorks, 1995.

[24] H. Kajiwara, P. Apkarian, and P. Gahinet, "Wide-Range Stabilization of an Arm-Driven Inverted Pendulum Using Linear Parameter-Varying Techniques," http://momiji98.ces.kyutech.ac.jp/publication.html, 1998.

Hiroyuki Kajiwara received the B.S. degree in Engineering from Kyushu Institute of Technology in 1975, the M.S. and Ph.D. degrees in Engineering from Tokyo Institute of Technology in 1977 and 1985, respectively. He was a research assistant at Tokyo Institute of Technology, 1977-1982, and an associate professor at Okayama University, 1982-1990. Since 1990, he has been an associate professor at Kyushu Institute of Technology. His research interest is computer-aided control system design and he is currently working on LPV modeling and control of an autonomous underwater vehicle.

Pierre Apkarian received the Engineer's degree from the Ecole Supérieure d'Informatique, Electronique, Automatique de Paris, in 1985, the M.S. degree and Diplôme d'Etudes Appronfondies in Mathematics from the University of Paris VII in 1985 and 1986, and the Ph.D degree in control engineering from the Ecole Nationale Supérieure de l'Aéronautique et de l'Espace (ENSAE) in 1988. Since 1988, he has been a research scientist at ONERA-CERT and associate Professor at ENSAE. His research interests include robust and gain-scheduling control theory, linear matrix inequality techniques, mathematical programming and applications in aeronautics. He is a member of IEEE and SIAM.

Pascal Gahinet graduated from the Ecole Polytechnique in 1984 and from the E.N.S.T.A., Paris, France, in 1986, and received the M.S. degree (electrical and computer engineering), and the Ph.D. degree (system theory), from the University of California, Santa Barbara, in 1987 and 1989, respectively. He was with the French National Research Institute in Computer and Control Sciences (I.N.R.I.A.) from 1990 to 1995, taught control at E.N.S.T.A. from 1991 to 1994, and also served as a consultant for THOMSON-CSF and Aérospatiale. He has been with The MathWorks Inc. since April 1996, and is currently senior project leader for the control and advanced control product developments. His research interests include robust control theory, linear matrix inequalities, numerical linear algebra, and numerical software for control. He is co-author of the *LMI Control Toolbox* and the *Control System Toolbox* for use with *Matlab*.